Chapter 11
II–VI Semiconductor-Based Humidity Sensors

Ghenadii Korotcenkov, Michail Ivanov, and Vladimir Brinzari

11.1 Introduction in Humidity Measurements

Due to the unique properties of water, humidity strongly affects living organisms, including humans, and materials [30]. Water molecules in the air change the length of organic materials, the conductivity and weight of hygroscopic materials and chemical absorbents, and the overall resistance of virtually any material. It changes the color of chemicals, the refractive index of air and liquids, the speed of sound in air or electromagnetic radiation in solids, and the thermal conductivity of gases as well as liquids and solids [58]. The efficiency and safety of many manufacturing processes, including the production, drying and storage of paint, paper, matches, furs, leather, wood products, foodstuffs, pharmaceuticals, ceramics, printing materials and semiconductor devices, are also highly dependent on the level of humidity in the surrounding atmosphere. Moreover, the industries mentioned above are just a few of the industries that need to control humidity. The amount of water vapor in the air also affects our safety, human comfort and quality of life, health, and living conditions of all living organisms, including microorganisms. In agriculture, the measurement of humidity is important for the plant protection (dew prevention), the soil moisture monitoring, etc. In the medical field, a humidity control should be used in respiratory equipment, sterilizers, incubators, pharmaceutical processing, and biological products.

Humidity measurements at the Earth's surface are also required for meteorological analysis and forecasting, climate studies, and for many special applications in hydrology, aeronautical services, and environmental studies, because water vapor is key agent in both weather and climate. As is known, water vapor is the most abundant greenhouse gas. Along with other greenhouse gases, water vapor is transparent

G. Korotcenkov (✉) · M. Ivanov · V. Brinzari
Department of Physics and Engineering, Moldova State University, Chisinau, Moldova

to most solar energy. However, at the same time water vapor absorbs the infrared energy emitted upward by the earth's surface, preventing the earth from cooling at night. However, it should be borne in mind that air humidity is not constant. Changes in the water vapor content in the atmosphere not only varies with the time of day and latitude but also is affected by seasonal changes. The amount of water vapor in the air also depends on the air temperature, and this change can occur in a very wide range. Therefore, to predict changes caused by humidity, humidity control becomes mandatory in all areas of our activities, from meteorological observations and industrial control to create comfortable conditions for our lives and understand the nature of changes in the climate [16, 31, 46, 50, 53, 54, 59].

People began to realize the importance of the process of measuring humidity many years ago. Back in the fifteenth century, Leonardo da Vinci built the first device to measure air humidity. According to other sources, the German Nicolaus de Cusa invented the first hydrometer in the same fifteenth century. It was wool gravimetric *hygrometer.* There is also evidence that accurate measurement of relative humidity was very important even in ancient China and Japan [22].

Currently, many different devices, using different principles, have been developed to measure the level of relative humidity (RH) [31, 32]. For example, there is a variety of optical hygrometers, fiber-optic and planar optical humidity sensors [31]. However, in this chapter we will only consider solid-state II–VI semiconductor-based sensors operating on the basis of electrical and electronic principles [32, 46, 50, 54]. These devices, first of all, include capacitance-, conductometric-, and mass-sensitive humidity sensors. It is important to note that for the development of humidity sensors based on II–VI semiconductors, the most stable ZnS, ZnSe, and CdS compounds were mainly used. Goodell et al. [19] have shown that even ZnS nanoparticles (~3 nm) in humid atmosphere are stable at low temperatures. At a high humidity level close to 100% RH, structural changes become noticeable only after prolonged treatments (18 h) at temperatures~50 °C. Goodell et al. [19] believe that at these temperatures, increased surface coverage with water allows the nanoparticles to rearrange within the aggregate, creating more contacts between the particles. These additional contacts provide an additional mechanism to reduce surface energy and stabilize the more crystalline structure.

11.2   General View on the Mechanisms of Humidity Sensing

Unfortunately, the interface of water and the II–VI compounds is not well understood yet, which makes it difficult to understand the processes occurring on the surface of these compounds when interacting with water vapor. We found only a few direct experimental reports on water adsorption on II–VI semiconductor surfaces [20, 24, 26, 62, 63]. We also found several publications presenting the results of theoretical modeling of the processes of interaction of water molecules with the ZnS surface [5, 39, 63] and CdS [21]. However, given that the principles of operation of gas sensors based on metal oxides and II–VI semiconductors are identical, it

can be assumed that the mechanisms of humidity sensing for these materials will also be identical. Other developers of II–VI semiconductor-based humidity sensors [7, 61] share the same opinion. This is quite understandable, since metal oxides formally refer to II–VI compounds in terms of their electronic and chemical properties.

According to existing concepts, the sensor response to water vapor is due to three processes, which are chemisorption, physisorption, and capillary condensation of water vapor [14, 32–34]. The chemisorption effect dominates at low humidity levels, and is manifested in the formation of OH groups on the surface of solids with a corresponding electronic exchange between chemisorbed particles and the bulk of the semiconductor. As in metal oxides, the OH group on the stoichiometric surface of chalcogenides is bonded to the metal atom, and a hydrogen, as a proton, is bonded to the surface chalcogen atom [60]. FTIR measurements performed by Goswami and Sen [20], experimentally supported this statement. They believe that S–H and Zn–O bonds are dominated on the surface of ZnS after water interaction with ZnS. With a further increase in the level of humidity and the formation of a continuous layer of OH groups, physisorption begins to dominate, which manifests itself in the formation of a multilayer of water, where both H^+ and H_3O^+ act as charge carriers [42, 43]. At the stage of chemisorption, a change in conductivity can be associated with both a change in the surface potential of crystallites and the height of the intercrystalline potential barrier, which limits the flow of current in polycrystalline materials, and surface migration of protons, carried out by hopping from site to site across the surface. When the surface is covered by water, proton transport is predominant. The results of research carried out by Choudhari et al. [7] are direct confirmation of the ongoing changes in the mechanism of conductivity with a change in humidity. By studying the impedance of ZnSe films in the range of 20–100% RH, they found that at low levels of relative humidity, the impedance is purely resistive, while at high levels of relative humidity, the impedance is purely capacitive. According to Choudhari et al. [7], at high humidity, water molecules condense in intergrain space, and therefore, ZnSe films behave like an electric two-layer capacitor.

As for the capillary condensation of water vapor, the role of this process in changing the properties of the material increases sharply in the presence of pores in these materials, especially in the nanometer range [1]. It was found that in the presence of narrow capillaries, vapor condensation occurs at pressures below the normal saturated vapor pressure. The Kelvin radius characterizes the critical size of pores for a capillary condensation effect. In the case of water, the condensation of vapor into the pores can be expressed by a simplified Kelvin equation [49]:

$$r_K = \frac{2\gamma V_M \cos\theta}{\rho RT \ln(\%RH/100)},$$

(11.1)

where γ is the surface tension of vapor in the liquid phase, V_M is molecular volume, θ is contact angle, and ρ is the density of vapor in the liquid phase. In this

equation, the thickness of the adsorbed layer was ignored. It is seen that the Kevin radius increases with the relative humidity, and the rate of change (the slope) increases with relative humidity as well. This means that the pores with smaller diameter are filled first, while bigger pores are filled later. At that the larger the θ, the larger the Kevin radius.

11.3   II–VI-Based Humidity Sensors

11.3.1   Conductometric RH Sensors

Conductometric or resistive RH sensors in their design and principles of operation are almost identical to conductometric gas sensors, discussed in previous Chapters. The only difference is the operating temperature. Conductometric RH sensors generally operate at room temperature. The main results related to the study of conductometric RH sensors developed on the basis of II–VI compounds are shown in Table 11.1.

Analyzing the results presented in Table 11.1, we can conclude that in the development of humidity sensors based on II–VI compounds, all approaches used in the development of sensors based on metal oxides were used. As can be seen from Table 11.1, sensors based on films formed by thick-film technology [7, 9, 25, 37, 61], individual nanowires (NWs) [12, 28], NWs array [25, 36, 40, 47, 56, 64], and composites [6] were tested. There have been also attempts to develop paper-based sensors [3, 23].

11.3.1.1   Thin Film RH Sensors

Naturally, the simplest way to manufacture humidity sensors is to form a sensitive layer on a dielectric substrate using the thick-film technology. The experiment has shown that for the synthesis of nanoparticles used for preparing humidity-sensitive layer, a variety of methods can be used, from hydrothermal synthesis [7, 37] to chemical bath deposition [9, 25] and co-precipitation [3, 6]. Sensors manufactured using this approach, regardless of the synthesis technology of II–VI semiconductor nanoparticles (NPs) used, have demonstrated high sensitivity. For most sensors, when the humidity changes in the range of 20–95% RH, the resistance changes up to $3 \cdot 10^3$ times (see, for example, Fig. 11.1a). The best sensor samples also demonstrated fast response and recovery after contact with water vapor (Table 11.1). Further testing after additional measurement cycles demonstrated good reproducibility of the sensor response (Fig. 11.1b). These are good parameters for conductometric-type humidity sensors [31, 32], which testify that the electrical response of II–VI semiconductor nanoparticles is very sensitive to changes in humidity, and these materials can indeed be used to develop humidity sensors.

Table 11.1 Parameters of conductometric humidity sensors based on II–VI semiconductor compounds

Material	Method	Structure	RH, %	R_0, Ohm	S, R_0/R_{RH}	τ_{res}/τ_{rec}, s	References
ZnS:Au, sphere ($D \sim 200$ nm; t-10–20 nm)	HT	Film	11–95	N/A	45	~18/30	[37]
ZnS NPs ($t \sim 50$ nm)	CBD	Film	30–95	$8 \cdot 10^9$	~10^2	N/A	[25]
ZnSe NR ($d \sim 200$ nm; $l \sim 1$–2 μm)	SSCR	Film	20–85	$3 \cdot 10^9$	~$4 \cdot 10^2$	50/80	[61]
ZnSe NPs ($t \sim 7$–21 nm)	HT	Film	20–100	~10^9	~10^3	8/13	[7]
CdS NPs	CBD	Film	15–85	~10^{11}	~$5 \cdot 10^2$	60/30	[9]
CdSNPs ($t \sim 3$ nm)	CP	Film, composite CdS-PANI	11–95	~10^5	~10^4	8/–	[6]
ZnS:Cu (1%) NPs	Pur.	Film, ZnS:Cu/paper	30–90	N/A	~1.3	180/150	[23]
CdS NPs ($t \sim 3$ nm)	CP	Film, CdS/ paper	5–99	N/A	~1.5	55/–	[3]
ZnS NWs ($d \sim 120$–160 nm)	VLS	NWs array	33–84	$3 \cdot 10^3$	~10^3	14/8	[56]
ZnS NWs ($d \sim 60$–120 nm)	VLS	NWs array	30–97	N/A	$3 \cdot 10^3$	N/A	[47]
ZnSe NWs	TcE	NWs array	10–95	$2 \cdot 10^9$	~10^3	<10/10	[36]
CdSSe NWs	CVD	NWs array	25–80	~10^6	~2	N/A	[40]
CdSSe NWs	CVD	NWs array	25–80	$2 \cdot 10^7$	~4	N/A	[64]
ZnS:Al NWs ($d \sim 60$–120 nm)	TcE	Ind-NW	50–90	$2 \cdot 10^6$	$2 \cdot 10^2$	N/A	[28]
CdS NW ($d \sim 50$–150 nm)	CVD	Ind-NW	30–90	~$5 \cdot 10^6$	~10^2	1.5/2.5	[12]

CBD chemical bath deposition, *CP* chemical precipitation technique, *CVD* chemical vapor deposition, *d* diameter of the nanowires, *D* diameter of the spheres, *HT* hydrothermal, *Ind-NW* individual NW, *l* length, *N/A* not available, *NR* nanorod, *NW* nanowire, *PANI* polyaniline, *Pur.* Purchased, *SSCR* solid-state chemical reaction, *t* crystallite size, *TcE* thermal co-evaporation method, *VLS* vapor–liquid–solid

Only sensors based on ZnS spheres synthesized by the hydrothermal method, despite the small size of the crystallites that form the spheres, had a noticeably lower sensitivity to humidity. Based on the analysis of TEM images of the ZnS spheres, which are an agglomeration of densely packed crystallites, it can be assumed that exactly this specific structure of nanospheres is the reason for such behavior of humidity sensors. Due to the dense structure of the sphere walls, "dead" zones are formed inside them, which do not participate in interaction with water vapor. In this regard, only crystallites from the outer layer participate in the gas-sensing effect. This means that the sensitive layer is too thin to make a significant
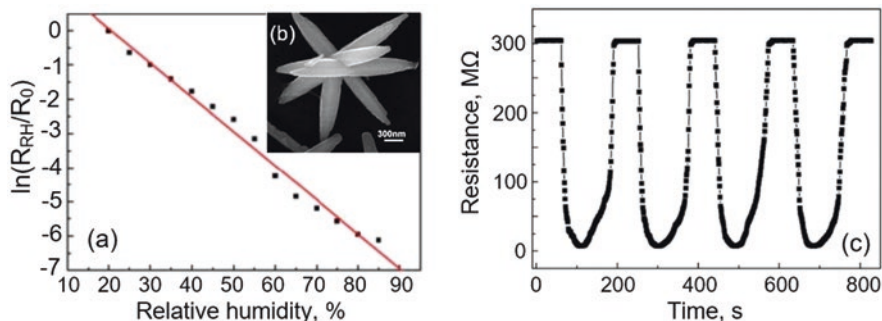
Fig. 11.1 (**a**) Static and (**c**) dynamic conductometric responses of ZnSe nanorod-based films to humidity, (**b**) SEM image of ZnSe nanorod. (Reprinted with permission from Yan et al. [61]. Copyright 2009: Elsevier)
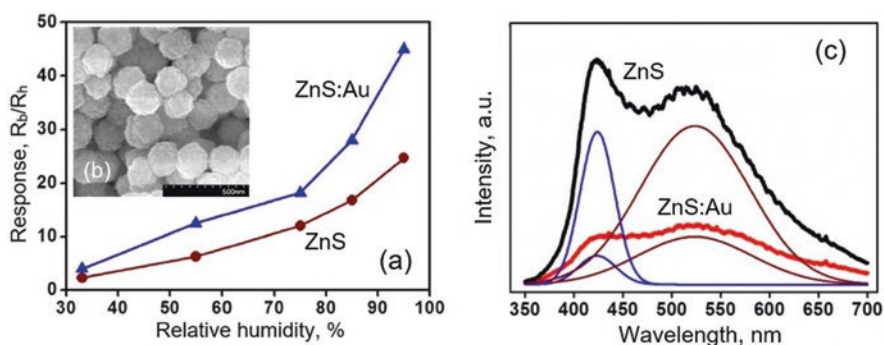

Fig. 11.2 (**a**) Humidity-sensing responses of the ZnS and ZnS-Au sphere-based sensors, (**b**) SEM image of ZnS nanospheres with diameter ~ 200 nm. (**b**, **c**) PL spectra of the ZnS and ZnS-Au spheres. Each PL spectrum was divided by two Gaussian deconvolution curves, which were centered at approximately 425 nm (blue line) and 525 nm (brown line). (Reprinted from Liang and Liu [37]. Published2014 by Springer as open access)

contribution to the change in the conductivity of the sensitive layer formed by the nanospheres. Surface modification by noble metals can improve the sensitivity of these sensors (Fig. 11.2a). In particular, Liang and Liu [37] established that the ZnS:Au sensors exhibited twofold increase in sensitivity compared with sensors based on a pure ZnS nanocrystalline spheres. Unfortunately, the authors did not offer an acceptable description of the mechanism of the observed sensing of sensors. The studies carried out do not answer the question – how do gold clusters on the ZnS surface affect the proton conductivity of the surface layer? There is only an assumption that the observed changes are associated not with the appearance of gold clusters, but with the peculiarity of the used process of its deposition. It is possible that it is the process of plasma sputtering used to deposit gold can damage the ZnS surface to a certain extent, and thus alter the surface characteristics of the ZnS, involved in interaction with water vapor. This assumption is confirmed by the change in the photoluminescence spectrum after the deposition of gold (Fig. 11.2b).

Thin film humidity sensors also include sensors developed by Hsueh et al. [25]. They have integrated ZnS thin film humidity sensors with $MgF_2/ZnS/CuIn_{1-x}Ga_xSe_2$ (CIGS)/Mo photovoltaic cell to create the so-called self-powered device. Its structure and connections between elements of the sensor are showed in Fig. 11.3. Soda-lime glass (SLG) was used as a substrate. Both ZnS layers of this double-sided device were deposited simultaneously by chemical bath deposition method at 80 °C. All interdigitated electrodes were deposited on the back of the ZnS film by sputtering. 100-nm-thick MgF_2 was also deposited on the top of the photovoltaic (PV) cell as the anti-reflection layer by thermal evaporation.

Testing of the developed devices has shown that the backside ZnS humidity sensor can function using power from the front CIGS *photovoltaic (PV)* cell. The curve in Fig. 11.4 reflects the effect of humidity on the sensor readings under illumination corresponding to 1 sun. Repeated measurements showed good reproducibility of the sensor response. The measured currents were very stable with negligible fluctuation. This suggests that the developed device is indeed a self-powered humidity sensor. However, when the illumination changes in the range of 1–0.1 of sun illumination, the signal decreases almost threefold (Fig. 11.4). It was found that the observed change is a consequence of the change in the open-circuit voltage (V_{oc}). When changing solar illumination from 1 sun to 0.8, 0.6, 0.4, 0.2, and 0.1 sun, V_{oc} varied from 0.6 to 0.59, 0.58, 0.57, 0.55, and 0.52 V, respectively. Since, due to the high resistance of the ZnS film (10^7–10^9 Ohm), the PV cell operates in open-circuit mode, the sensor supply voltage corresponds to V_{oc}. Therefore, due to the change in V_{oc}, the measured currents also changed. True, the change in sensor signal significantly exceeds the change in open-circuit voltage. In all likelihood, in the course of measurements, illumination of the humidity sensor also occurs, contributing to the change in the resistance of the ZnS film. It follows that for correct humidity measurements, it is necessary not only to control the sensor resistance and the open-circuit voltage of the PV cell but also to use some calibration curves that take into account the effect of lighting on the sensor readings. This creates certain difficulties for the use of such sensors.
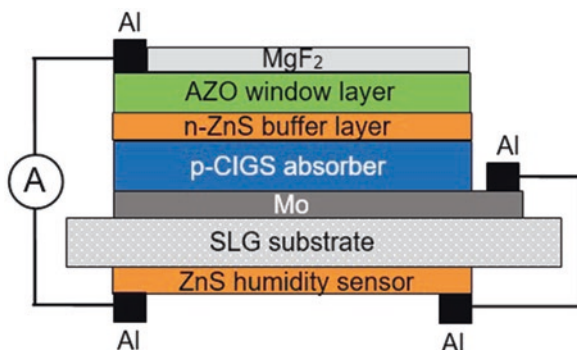

Fig. 11.3 Schematic diagram of the bifacial self-powered device with an integrated CIGS PV cell and ZnS humidity sensor. (Idea from Hsueh et al. [25])
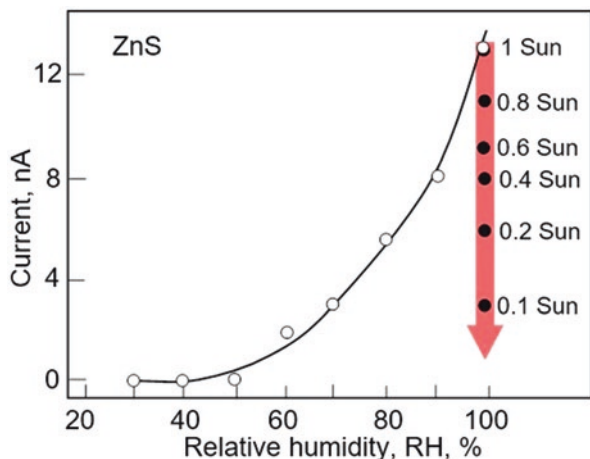
Fig. 11.4 The current measured at RH 95% with varied illumination. (Data extracted from Hsueh et al. [25])
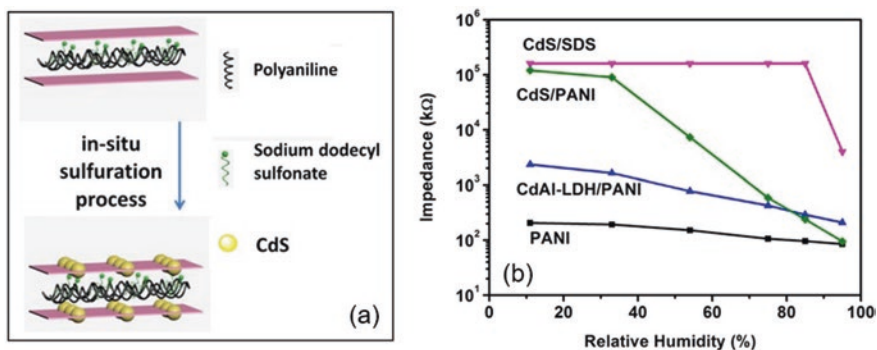

Fig. 11.5 (**a**) Schematic illustration of the transformation from the CdAl-LDH to the CdS. (**b**) Response of the sensors of CdS/PANI, CdS/SDS, CdAl-LDH/PANI, and PANI to humidity: *SDS* sodium dodecyl sulfonate, *CdAl-LDH* co-intercalated Cd, Al layered double hydroxides. (Reprinted with permission from Chen et al. [6]. Copyright 2018: Elsevier)

As for the most sensitive humidity sensors based on 2–6 compounds and fabricated as the thin films, such sensors are devices developed by Chen et al. [6]. The main element of these sensors is the layers of CdS/PANI composite with sandwich structure (Fig. 11.5a). CdS/PANI composite was synthesized by in situ sulfuration process of polyaniline (PANI) and sodium dodecyl sulfonate (SDS) co-intercalated Cd, Al layered double hydroxides (CdAl-LDH/PANI). Sensors based on CdS/PANI composite showed good sensitivity to humidity, low hysteresis (0.5% under 54% RH) (Fig. 11.6b), and fast response/recovery processes compared with PANI-based sensors. When the relative humidity increased from 11% to 95%, the impedance quickly decreased by four orders of magnitude after just 8 s and response improved by three orders of magnitude compared to pure PANI (see Fig. 11.6b). It is also
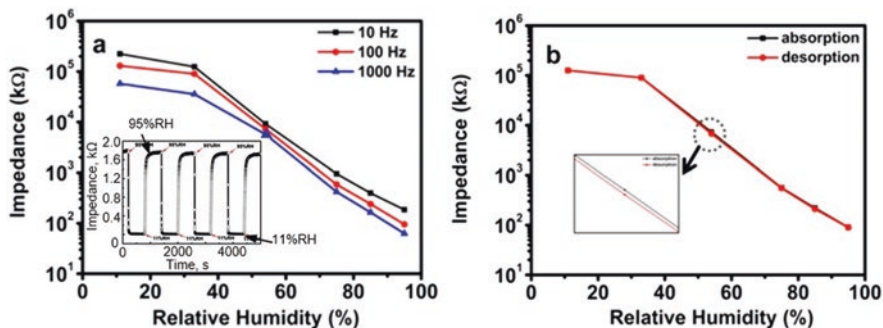
Fig. 11.6 (**a**) The impedances of sensor based on CdS/PANI varied with a humidity series at different frequencies and the insert plots the repeated response and recovery characteristics of CdS/PANI composite; (**b**) Humidity hysteresis of CdS/PANI sensor at the working frequency of 100 Hz. (Reprinted with permission from Chen et al. [6]. Copyright 2018: Elsevier)

important to note that the logarithmic impedance of the CdS-PANI layer formed on the Ag-Pd interdigitated electrodes was linear with respect to relative humidity and had a weak frequency dependence, as well as good repeatability in cyclic tests (Fig. 11.6a).

According to Chen et al. [6], reported characteristics of CdS/PANI-based humidity sensors are attributed to the unique construction of CdS/PANI composite, which can form orderly interwoven network structure between CdS and PANI. At that sensor response of such a structure mainly arises from the interaction of water vapor with PANI. Polyaniline (PANI) is conjugated conducting polymer that exhibits good conductivity and electrochemical reversibility. It was confirmed that the change in the conductivity of PANI under influence of humidity is associated with the "proton effect." Water is well known for its protonation, and the released proton interacts with universally conjugated C=C double bonds in polyaniline. The electrical conductivity of PANI under the influence of water vapor can be viewed as a jump of electrons, which is facilitated by the exchange of protons. Chen et al. [6] believe that sandwich construction of composite is favorable for enhanced mobility of the anion or the charge transfer across the polymer chains. In addition, the sandwich structure provides polymer molecules with a confined and stable environment, which improves humidity and thermal stability [6].

11.3.1.2 Nanowire-Based Sensors

Currently, the use of 1D nanostructures in the development of various devices is a very popular direction. As can be seen from the results presented in Table 11.1, 1D nanostructures are also used in the development of II–VI semiconductor-based RH sensors. The main result of these studies is confirmation of the fact that the use of both individual nanowires (NWs) and an array of NWs helps reduce response and recovery times, as well as hysteresis. For example, Du et al. [12] reported that their humidity sensors based on individual CdS nanowires had response and recovery times ~1.3 and 2.4 s, correspondingly. It should be noted that the same situation was

observed for humidity sensors based on the metal oxide 1D nanostructures [17]. High gas permeability in the absence of nanopores is the main explanation for the observed effect. Fast response is an important advantage of NW-based RH sensors. The absence of pores in 1D structures also excludes the possibility of capillarity condensation of water vapor, which allows such sensors to operate at very high humidity levels. However, the absence of intercrystalline barriers and nanopores in such structures leads to the fact that the noticeable sensitivity to humidity in these devices is shifted toward higher humidity levels in comparison with traditional sensors based on nanocrystalline materials. These statements are clearly visible in Fig. 11.7, where the results, obtained by Okur et al. [47], are presented for ZnS nanowire-based humidity sensors. The sensors are capable of operating up to 97% RH, but an acceptable sensor response is only observed above 30% RH.

Nanowire-based sensors also show good repeatability (Fig. 11.8b). However, as noted in Korotcenkov [34], with the existing technology for growing 1D structures, one cannot expect good reproducibility of the sensor parameters. This is confirmed by the results given in Fig. 11.8a. It can be seen that the resistance of individual nanowires varies within a fairly wide range. This variation in parameters creates additional difficulties when replacing sensors in real devices used in different applications.

Zhang et al. [64] and Lu et al. [40] tried to optimize the structure of nanowire-based humidity sensors (Fig. 11.9a). However, their attempts were not successful. Given the specific properties of polyimide (PI), such as high temperature resistance, good mechanical and adhesive properties, good chemical resistance, low dielectric constant, long-term stability in the presence of moisture, and insulation, Zhang et al. [64] and Lu et al. [40] proposed to apply polyimide to the surface of the CdSSe nanowire array (Fig. 11.9c). As a result, they obtained the structure shown in Fig. 11.9d. The humidity-sensing response of these sensors is shown Fig. 11.9e. The manufactured sensors showed a linear dependence of resistance on humidity and a
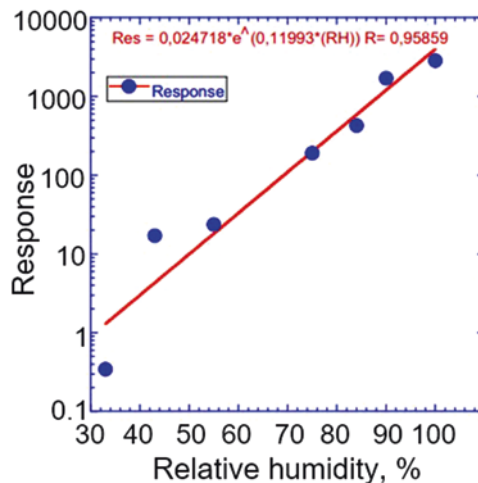

Fig. 11.7 Variation in sensor values of ZnS nanowires versus 22%, 33%, 43%, 55%, 75%, 84%, and 97% RH. (Reprinted with permission from Okur et al. [47]. Copyright 2012: Elsevier)
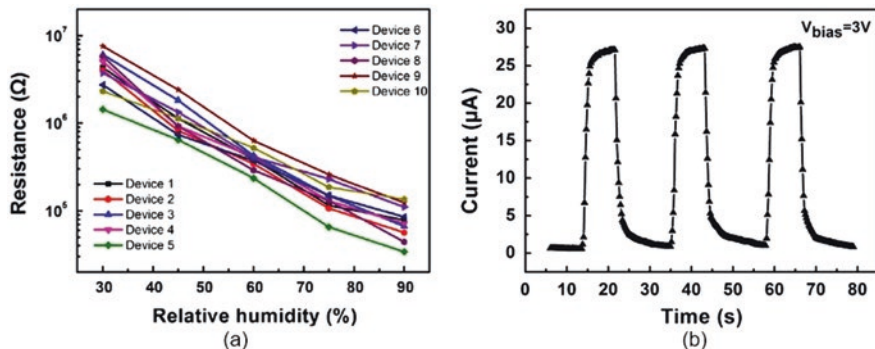
Fig. 11.8 (**a**) Relative humidity influence on the resistances of sensors based on the individual CdS nanowire for ten devices; (**b**) Current response of a CdS NW sensor to dynamic switches between dry air (5%) and moist air of 75% RH at V_{bias} = 3 V. The CdS NWs were synthesized via a CVD method in a Cd-enriched atmosphere. The CdS NWs had the diameter in the range of 50–150 nm and the length of typically tens of micrometers. (Reprinted with permission from Du et al. [12]. Copyright 2014: Elsevier)
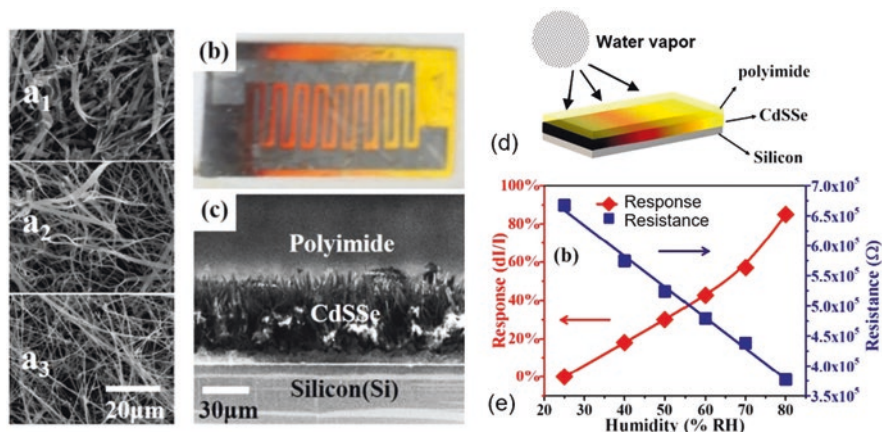

Fig. 11.9 (**a**) (a_1–a_3) the SEM images of CdSSe nanowire array chips. Scale bar: 20 μm. (**b**) The image of the humidity sensor with interdigital electrodes. (**c**) Cross-sectional SEM image of PI coated CdSSe nanowire chip. Scale bar: 30 μm. (**d**) Schematic diagram of the sensor; (**e**) The humidity-sensing response and sensor resistance at different relative humidity values. (Reprinted from Lu et al. [40]. Published 2019 by IOP as open access)

fairly good stability of characteristics. The resistance of the sensors, regardless of the humidity level, was stable for 1000 s. However, the magnitude of the sensor response was significantly less than that of sensors with an open surface of the CdSSe nanowire array (see Table 11.1). Sensor response appears to have been very slow too.

According to the authors of these articles, the functional layer for humidity monitoring is PI, which, due to the expansion caused by humidity in the PI layer, puts

pressure on the conductive layer of the nanowire, causing a change in its conductivity and thus provides humidity measurement. In principle, this mechanism of sensitivity to humidity is realistic, since swelling of the PI occurs in a humid atmosphere [51]. According to Sager et al. [51], a humidity extension coefficient is only 60–80 ppm/%RH. However, it is not known if this expansion is sufficient for the observed effect to occur, since it is not clear how this expansion will affect the underlying layer of NWs array. Besides, experiments carried out by [2] showed that only an amount of 1.5–6% water (by mass) can be absorbed by the polymer material in 100% RH air. That is, the change in PI film weight is also not significant. It should also not be forgotten that polyimide, depending on the manufacturing technology, can have good permeability for gases and water vapors. Therefore, the very effect of the sensitivity to humidity of sensors developed by Zhang et al. [64] and Lu et al. [40] may be a simple consequence of the permeability of the polyimide. In this case its small value only indicates that the polyimide coating, due to its low permeability, significantly limits the penetration of water vapor to the CdSSe nanowire array.

11.3.1.3   Paper-Based RH Sensors

He et al. [23] and Bhattacharjeea et al. [3] suggested an interesting approach to developing flexible humidity sensors. For the manufacture of sensors, they used filter paper on which CdS [3] or ZnS:Cu [23] nanoparticles were applied by drop casting or spin coating. Previously, this approach has already been used in the development of gas and humidity sensors [18, 29, 41, 45]. He et al. [23] have shown that paper-based sensors have excellent flexibility and can operate under different bending conditions (see Fig. 11.10). However, such sensors, regardless of their design features and the material used, had low sensitivity and long response and recovery times. The reasons for the low sensitivity even when using CdS NPs with a size of ~3 nm are not explained by the authors. It can only be assumed that this behavior is associated with the influence of the paper used as a substrate, or with design flaws
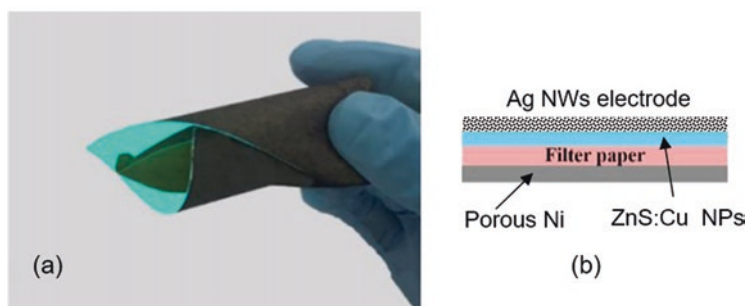

Fig. 11.10 (**a**) Schematic image of the paper-based sensor, (**b**) Image of изогнутого сенсора fabricated on the paper. (Reprinted from [23]. Published 2019 by MDPI as open access)
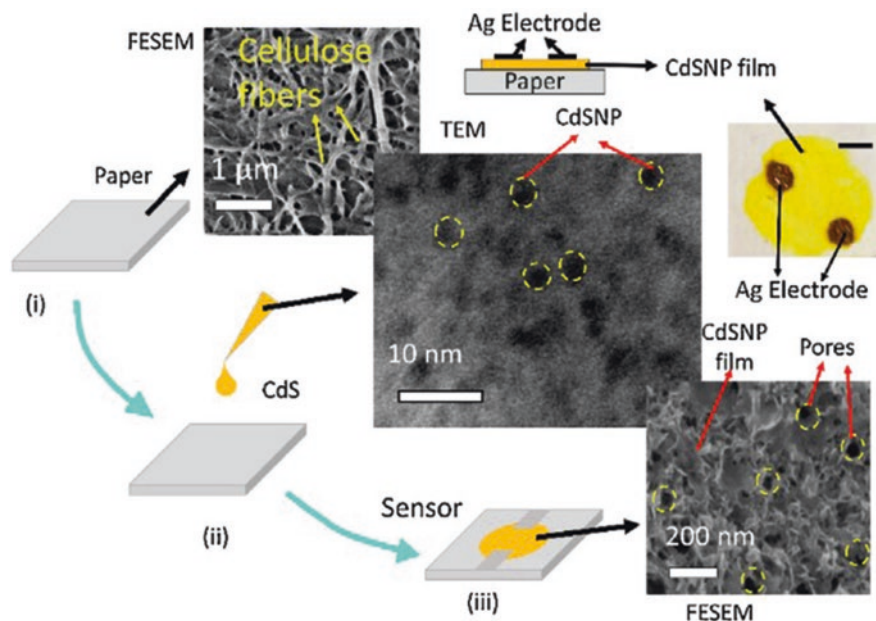
Fig. 11.11 Image (**a**) of this figure shows the fabrication steps (i–iii) of the sensor along with the FESEM image of the paper surface, TEM image of the CdSNPs, a cross-sectional schematic diagram along with a photographic image of the sensor, and a FESEM image of the paper embedded with CdSNPs. The scale bar in the sensor image is of 1.5 mm. (Reprinted with permission from Bhattacharjeea et al. [3]. Copyright 2019: Elsevier)

in the manufactured sensors. In one case (see Fig. 11.10a), the resistance of the paper makes a significant contribution to the total resistance of the sensor, sharply limiting the change in resistance of the sensor in a humid atmosphere. In another case (Fig. 11.11), due to the special structure of the paper, CdS nanoparticles do not form a continuous layer necessary to create a channel for the flow of charge carriers, which is controlled by the properties of only CdS nanoparticles. It should not be forgotten that the paper itself is involved in the processes of adsorption and desorption of water vapor and can significantly affect the response kinetics of sensors developed using layers of II–VI semiconductor compounds formed on its surface.

11.3.2 Capacitance RH Sensors

In the simplest case, a capacitance-type sensor is made of two parallel plates. In such structure the capacitance between the two electrodes is given by equation

$$C = \varepsilon_r \varepsilon_0 \frac{A}{d},$$

$$(11.2)$$

where ε_r and ε_0 are the relative and vacuum permittivity constants, respectively, A is the plate surface area, and d is the plate distance. From this equation, it is evident that only three ways exist to effect a change in the capacitance of that device: (1) alter the distance d between the two plates, (2) alter the overlapping area A between the two plates, and (3) change the dielectric permittivity between the plates [27]. This means that capacitive sensors can detect only those gases and vapors that affect these parameters. In principle, water vapor when interacting with various materials can exert such influence. In particular, the filling of pores in sensing material with water during its condensation can give rise to a multiple increase in the dielectric constant at the corresponding porosity of the material. As is known, the dielectric constant of air is 1 and that of water is 81. The dielectric constants of CdS and ZnS are ~9–10. That is why, by measuring the change in capacitance, it is possible to determine the presence of water vapor in the air. The principles of operation and a more detailed description of the design of capacitive gas and humidity sensors can be found in Ref. [4, 27].

Parameters of capacitance RH sensors based on II–VI compounds are listed in Table 11.2. It is seen that all these sensors were developed using metal oxide-based composites [15, 44, 48]. Their testing showed that the highest capacitance response (C_{RH}/C_0) was possessed by sensors based on CdS-ZnO heterostructures with a specific structure formed on the basis of silicon nanoporous pillar array (NPA) (see Fig. 11.12). ZnO nanorods were formed using chemical vapor deposition (CVD) method, and CdS nanoparticles with average diameter of ~70 nm were synthesized using successive ion layer adsorption reaction (SILAR) method. With a change in humidity in the range of 3–95%, the capacity of such sensors changed by more than $2 \cdot 10^3$ times (Fig. 11.13a). The results also show that the response of the sensor prototypes decreases with increasing frequency. It may be due to the comparability of the relaxation time of the related processes with the period of applied measuring AC voltage. According to Feng et al. [15], fast response/recovery times and low hysteresis of CdS/ZnO/Si-NPA-based sensors were attributed to the combined effect of the channel network created by Si-NPA (see Fig. 11.12a), which provided an efficient path for the penetration and removal of water vapor from the sensitive layer, and the physical and chemical properties of CdS, which facilitate adsorption/ desorption processes.

Table 11.2 Parameters of capacitance humidity sensors based on II–VI semiconductor compounds

Material	Method	RH, %	S (C_{max}/C_{min})	τ_{res}/τ_{rec}, s	References
CdS-ZnO	ZnO-CVD CdS-SILAR	3–95	~2000 (20 Hz)	110/32	[15]
CdSe-F8	CdSe (QDs)-chemical	10–95	~8 (120 Hz)	9/7	[44]
ZnS:Cu(1%)-PANI	ZnS:Cu - HT	30–90	~1.5 (N/A Hz)	42/24	[48]
ZnS:Cu(0.1%)-paper	ZnS:Cu – purchased	20–90	30 (10 kHz)	180/140	[23]

F8 polymeric semiconductor poly-(9,9-di-n-octylfluorenyl-2,7-diyl), *HT* hydrothermal method, *PANI* polyaniline
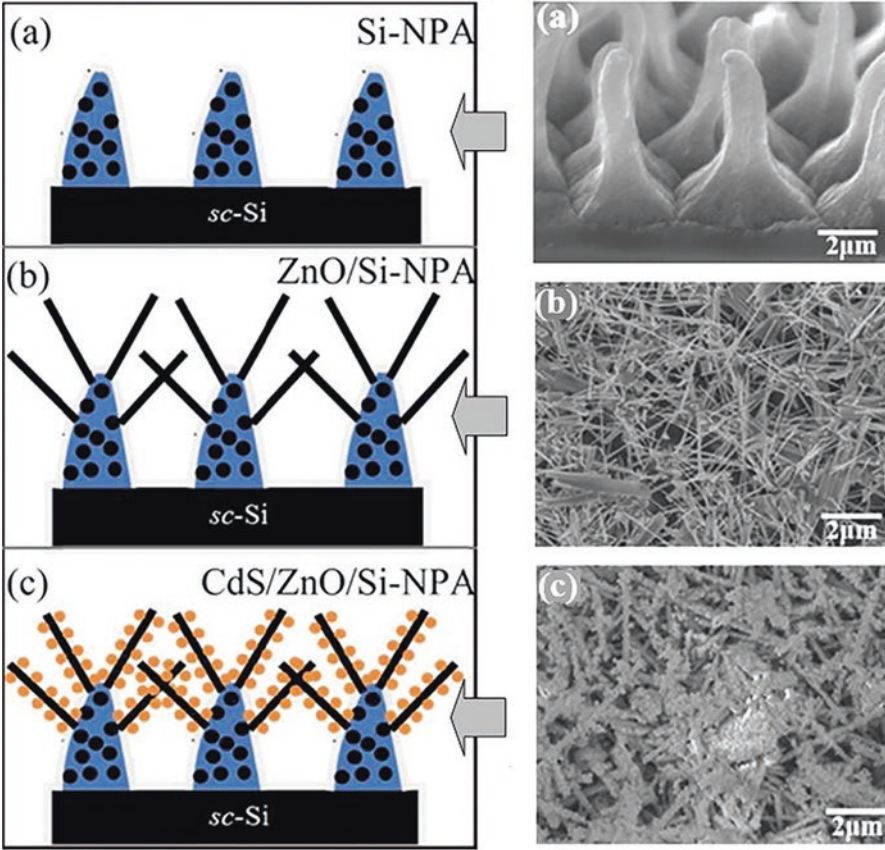
Fig. 11.12 The structural schematic diagrams and SEM images of (**a**) **Si-NPA, (b) ZnO/Si-NPA, and (c) CdS/ ZnO/Si-NPA. (Reprinted with permission from Feng et al. [**15**]**. Copyright 2017: Elsevier)

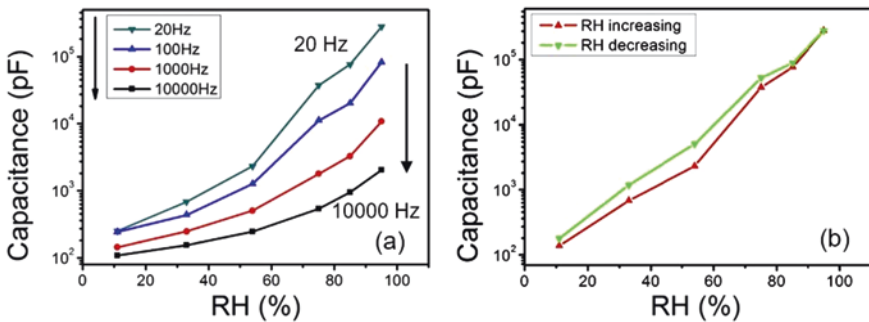**Fig. 11.13** (**a**) The capacitance variation of CdS/ZnO/Si-NPA with RH level measured with different frequencies. (**b**) The hysteresis of CdS/ZnO/Si-NPA between RH increasing and decreasing processes. (Reprinted with permission from Feng et al. [15]. Copyright 2017: Elsevier)

Table 11.3 Comparison of various parameters of capacitive humidity sensor based on polymer II–VI semiconductor composites

Material	C, pF		Sensitivity, $\Delta C/\Delta RH$ (pF/RH), %	Res./ Rec. time (s)	Hysteresis(%)	References
	30%RH	90%RH				
PANI	16	23.2	12	53/30	17.8	[48]
PANI/1% Cu-ZnS	18	25.1	12	42/24	1.5	
PANI/3% Cu-ZnS	22.1	24	3.2	47/29	2.7	
PANI/5% Cu-ZnS	21.6	23.2	2.5	55/30	2.9	
Ag/F8/Ag	16	65 (75%RH)	110	15/7	N/A	[44]
Ag/F8-CdSe/ Ag	12.1	89	116	9/7	~5	

As for the sensors based on polymer-based composites, their sensitivity to humidity was significantly lower. Moreover, given the concentration of CdSe and ZnS in the composite, at which some optimizing effect was achieved (see Table 11.3), II–VI compounds apparently do not determine the capacitive properties of the formed structures, but only affect the porosity of humidity-sensitive matrix. In this case, the polymer is the sensitive element in this matrix and its properties mainly determine the characteristics of humidity sensors. In particular, PANI is conducting/semiconducting stable polymer, the conductivity of which is largely dependent on its oxidation state. The increase in the capacity of capacitive moisture sensors based on PANI is mainly explained by an increase in the dielectric constant due to the absorption of water molecules, as well as by doping of PANI with water molecules. This doping, in addition to increasing the concentration of charges, also increases the polarizability of PANI.

11.3.3   QCM-Based RH Sensors

Quartz crystal microbalance (QCM) is a piezoelectric device based on the piezoelectric effect of materials. Typically, piezoelectric sensors are a quartz crystal disc coated on both sides with gold electrodes that serve as sensing surfaces. Quartz is the most commonly used piezoelectric material because of its low cost and stability against thermal, chemical, and mechanical stress. It was found that the quartz crystal microbalance technique is very sensitive to mass changes on the nanogram scale (~ 1 ng/cm^2) by measuring the change in the resonance frequency (Eq. 11.3). It responds to a given increase of mass simultaneously, regardless of the species adsorbed. Based on this, it can be concluded that these sensors are not selective. However, water in the range of commonly measured humidity levels (30–90% RH) can be adsorbed in much larger quantities than gases. Therefore, we can assume that QCM-based humidity sensors have some selectivity. The change in resonant

Table 11.4 Parameters of QCM-based humidity sensors developed using II–VI semiconductor compounds

Material	Method	Thickness	f_0, MHz	RH, %	Δf, Hz	τ_{res}/τ_{rec}	References
CdS NPs (30–40 nm)	CBD	200 nm	8	17–85	~1000	<6 min	[8]
ZnCdSSe NWs	CVD	NWs array	10	10–95	~1300	21/8 s	[55]
ZnS NWs (120–160 nm)	VLS	NWs array	8	30–100	~200	14/18 s	[56]
ZnS NWs (60–120 nm)	VLS	NWs array (100 nm)	8	22–97	~900	<50 s	[47]

CBD chemical bath deposition, *NPs* nanoparticles, *NWs* nanowires, *VLS* vapor–liquid–solid method

frequency depends on the change in mass of the sensitive layer (Δm) on the surface of the quartz crystal and can be calculated using the Sauerbrey linear frequency change relation [52]:

$$\Delta f = \frac{2 f_0^2 \Delta m}{A \sqrt{\mu \rho}}, \tag{11.3}$$

where f_0 is the resonant frequency of the fundamental mode of the QCM crystal, A is the area of the gold coated electrodes on the quartz crystal, ρ is the density, and μ is the shear modulus of the quartz substrate. Hence, it follows that the sensitivity of the sensors is determined by the adsorption properties of the material applied to the surface of the quartz crystal.

Quartz crystal microbalance (QCM)-based sensors are the most common type of mass-sensitive sensors used for both gas sensor [57] and biosensor applications [38]. The same situation is observed in the development of humidity sensors. Only QCM-based mass-sensitive sensors using II–VI compounds as sensitive layer have been tested as humidity sensors. The main parameters of these sensors are given in Table 11.4.

The results given in Table 11.4 indicate that QCM-based humidity sensors based on II–VI compounds have parameters suitable for practical use. It is seen that the change in the resonant frequency with a change in humidity in the range of 10–90% RH can exceed 1000 Hz. This means that the change in humidity in the specified range can be controlled with high accuracy.

An important result of these studies is also the confirmation of the significant role of the size effect in humidity sensing by QCM devices [55]. As is seen in Fig. 11.14, the sensor coated with ZnCdSSe NWs shows greater frequency shift than the others coated with thin film, nanosheets (NSs) and nanobelts (NBs). This is expected because the size of the NWs significantly less than the size of NSs and NBs (see, for example, Fig. 11.15). This means that such structures with the same weight of the sensitive layer have more of the specific and total surface, which creates the basis for greater water adsorption. The increase in sensor response with decreasing crystallite size or diameter of NWs, NSs, and NBs formed by the sensitive layer also correlates well with the conclusions drawn by Zhang et al. [63] in the process of analyzing the results of molecular dynamics (MD) simulations of the
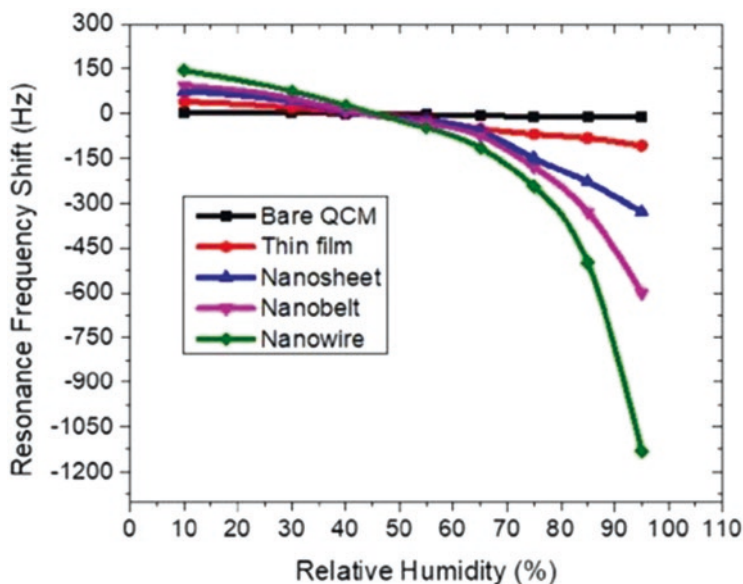
Fig. 11.14 Frequency shift response of different sensors fabricated with materials in different morphology respect to relative humidity of the environment. (Reprinted with permission from Turkdogan [55]. Copyright 2019: Springer)
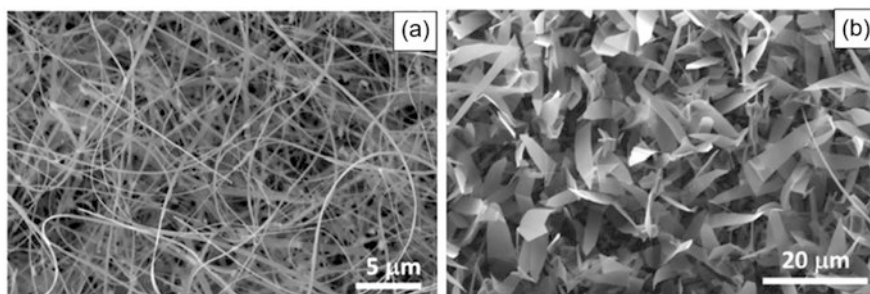

Fig. 11.15 SEM images of ZnCdSSe (**a**) nanowires and (**b**) nanosheets. (Reprinted with permission from Turkdogan [55]. Copyright 2019: Springer)

interaction between water molecules and zinc sulfide nanoparticles (3–5 nm). They concluded the followings. First, ZnS nanoparticles can adsorb more water molecules per unit of surface area because of the significantly increased curvature and more open surface configuration. Second, the water binding energy is higher in nanoparticles than in bulk crystals (although compared with isolated nanoparticles, aggregation can reduce the binding energy) because the intermolecular interaction of water on the curved nanoparticle surfaces is not as strong as in flat bulk surfaces. This means that a larger number of water molecules can be adsorbed by ZnS nanoparticles with a higher bond strength on the nanoparticle surface compared to bulk ZnS.
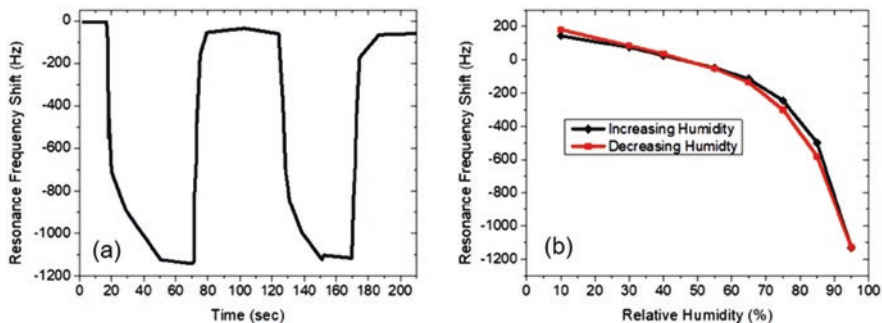
Fig. 11.16 (**a**) Repeatable sensing curve of the NW coated QCM gathered between ~95% RH and ~ 40% RH. (**b**) Hysteresis characteristic of NW coated QCM sensor. (Reprinted with permission from Turkdogan [55]. Copyright 2019: Springer)

Testing of sensors based on nanowires revealed another advantage of such sensors, which we noted when considering conductometric gas and humidity sensors. This advantage is high-speed performance. Figure 11.16b shows the response curve of the ZnCdSSe NW-based sensor as a function of time under the humidity levels of 40% RH and 95% RH. It was found that average response time of the sensor was around 21 s, while the recovery time was around 8 s in average. Such rates of response/recovery are very promising for practical application. They are not inferior to the best results described in the literature, or even surpass them (see Table 11.3). Okur et al. [47] also reported that their NW-based sensors were characterized by fast response and recovery.

Another promising characteristic of NW-based sensor is the small hysteresis. As shown in Fig. 11.16b, a hysteresis loop under increasing and decreasing humidity is only ~3% under 85% RH. This favorably distinguishes NW-based sensors from conventional capacitive humidity sensors based on porous materials, in which hysteresis is mainly associated with the processes of adsorption and desorption of water vapor from nanosized pores. As is known, there are no nanoscale pores in the NWs array.

In the manufacture of QCM-based humidity sensors based on II–VI compounds for the deposition of a sensitive layer on a quartz crystal, thick-film technology methods were usually used, such as immersion of gold coated QCM in the reaction solution [8], and drop casting method [47, 55, 56]. As a rule, after the deposition of a sensitive layer and its drying at room temperature, the formed layers were not further subjected to additional heat treatment to improve their adhesion to the metallized quartz substrate. This can be considered as a significant drawback of this technology, since in the absence of good adhesion, the sensitive layer may peel off during operation. Unfortunately, there are no data in the literature confirming the long-term stability of such sensors and thus refuting our statement.

11.4   Outlooks

If we compare humidity sensors based on II–VI semiconductor compounds with sensors developed on the basis of other materials [31–33], then we can state that their parameters do not differ much from the best samples. However, based on this, we have no right to assert that humidity sensors based on semiconductors II–VI will certainly appear on the humidity sensor market. Firstly, they cannot replace sensors already on the market, in particular metal oxide sensors, since the use of II–VI semiconductors does not improve performance and does not contribute to an increase in sensor selectivity compared to metal oxide sensors. Secondly, the parameters of II–VI semiconductor compounds are highly dependent on lighting and temperature, which complicates their operation. In addition, despite the high melting points, sublimation and especially irreversible oxidation occur at significantly lower temperatures [10, 11]. As a result, when operating such sensors, we cannot use heat treatment to restore the original characteristics of sensors after long-term operation, as can be done for metal oxide sensors [35]. The available information also does not provide grounds for asserting the long-term stability of the parameters of the sensors, especially when they are used in high humidity conditions. There is simply no such research. In most works, testing was limited to a time of no more than 20 minutes [64]. As a result, we do not know what processes can occur in II–VI semiconductor-based humidity sensors during operation, and how the aging effect will affect the parameters of the sensors. Too high resistance of ZnS and CdS can also create difficulties when using conductometric humidity sensors [13]. For example, sensors developed by Choudhari et al. [7] had resistance more than 10^9 Ohm.

References

1. Adamson AW, Gast AP. Physical chemistry of surface. New York: Wiley; 1997.
2. Bereir GA, Kline DE. Dynamic mechanical behaviour of polyimide. J Appl Polym Sci. 1968;12:593–604.
3. Bhattacharjeea M, Bandyopadhyay D. Mechanisms of humidity sensing on a CdS nanoparticle coated paper sensor. Sens Actuators A Phys. 2019;285:241–7.
4. Chatzandroulis S, Tserepi A, Goustouridis D, Normand P, Tsoukalas D. Fabrication of single crystal Si cantilevers using a dry release process and application in a capacitive-type humidity sensor. Microelectron Eng. 2002;61–62:955–61.
5. Chen H, Shi D, Qi J, Wang B. Electronic and mechanical properties of ZnS nanowires with different surface adsorptions. Phys E. 2009;42:32–7.
6. Chen Q, Nie M, Guo Y. Controlled synthesis and humidity sensing properties of CdS/polyaniline composite based on CdAl layered double hydroxide. Sensors Actuators B Chem. 2018;254:30–5.
7. Choudhari U, Jagtap S. Hydrothermally synthesized ZnSe nanoparticles for relative humidity sensing application. J Electron Mater. 2020;49:5903–16.

8. Demir R, Okur S, Seker M, Zor M. Humidity sensing properties of CdS nanoparticles synthesized by chemical bath deposition method. Ind Eng Chem Res. 2011;50:5606–10.

9. Demir R, Okur S, Seker M. Electrical characterization of CdS nanoparticles for humidity sensing applications. Ind Eng Chem Res. 2012;51:3309–13.

10. Dimitrov RI, Boyanov BS. Oxidation of metal sulphides and determination of characteristic temperatures by DTA and TG. J Therm Anal Calorim. 2000;61:181–9.

11. Dimitrov RI, Moldovanska N, Bonev IK. Cadmium sulphide oxidation. Thermochim Acta. 2002;385:41–9.

12. Du L, Zhang Y, Lei Y, Zhao H. Synthesis of high-quality CdS nanowires and their application as humidity sensors. Mater Lett. 2014;129:46–9.

13. Fang X, Zhai T, Gautam UK, Li L, Wua L, Bando Y, Golberg D. ZnS nanostructures: from synthesis to applications. Prog Mater Sci. 2011;56:175–287.

14. Farahani H, Wagiran R, Hamidon MN. Humidity sensors principle, mechanism, and fabrication technologies: a comprehensive review. Sensors. 2014;14:7881–939.

15. Feng MH, Wang WC, Li XJ. Capacitive humidity sensing properties of CdS/ZnO sesame-seed-candy structure grown on silicon nanoporous pillar array. J Alloys Compd. 2017;698:94–8.

16. Fleming WJ. A physical understanding of solid state humidity sensors. Soc Automot Eng Trans. 1981;90(2):1656–67.

17. Fu XQ, Wang C, Yu HC, Wang YG, Wang TH. Fast humidity sensors based onCeO_2 nanowires. Nanotechnology. 2007;18:145503.

18. Gimenez AJ, Luna-Barcenas G, Sanchez IC, Yanez-Limon JM. Paper-based ZnO oxygen sensor. IEEE Sensors J. 2015;15:1246–51.

19. Goodell CM, Gilbert B, Weigand SJ, Banfield JF. Kinetics of the water adsorption driven structural transformation of ZnS nanoparticles. J Phys Chem C. 2008;112(13):4791–6.

20. Goswami N, Sen P. Water-induced stabilization of ZnS nanoparticles. Solid State Commun. 2004;132:791–4.

21. Gupta SS, van Huis MA. Adsorption study of a water molecule on vacancy-defected on polar CdS surfaces. J Phys Chem C. 2017;121(18):9815–24.

22. Hattingh J. The importance of relative humidity measurements in the improvement of product quality. In: Proceedings of 2001 NCSL International Workshop & Symposium. 2001. http://www.ncsli.org/i/c/TransactionLib/C01_R7.pdf

23. He Y, Zhang M, Zhang N, Zhu D, Huang C, Kang L, et al. Paper-based ZnS:Cu alternating current electroluminescent devices for current humidity sensors with high–linearity and flexibility. Sensors. 2019;19:4607.

24. Hertl W. Surface chemical properties of zinc sulfide. Langmuir. 1988;4:594–8.

25. Hsueh H-T, Hsiao Y-J, Lin Y-D, Wu C-L. Bifacial structures of ZnS humidity sensor and Cd-free CIGS photovoltaic cell as a self-powered device. IEEE Electron Dev Lett. 2014;35(12):1272–4.

26. Huang F, Gilbert B, Zhang H, Banfield JF. Reversible, surface-controlled structure transformation in nanoparticles induced by an aggregation state. Phys Rev Lett. 2004;92:155501.

27. Ishihara T, Matsubara S. Capacitive type gas sensors. J Electroceram. 1998;2(4):215–28.

28. Jiang P, Jie J, Yu Y, Wang Z, Xie C, Zhang X, et al. Aluminium-doped n-type ZnS nanowires as high-performance UV and humidity sensors. J Mater Chem. 2012;22:6856.

29. Kannan PK, Saraswathi R, Rayappan JBB. CO_2 gas sensing properties of DC reactive magnetron sputtered ZnO thin film. Ceram Int. 2014;40:13115–22.

30. Korotcenkov G. Why do we need to control humidity? In: Korotcenkov G, editor. Handbook of humidity measurements, vol. 1: Spectroscopic methods of humidity measurement. Boca Raton: CRC Press; 2018. p. 17–45.

31. Korotcenkov G. Handbook of humidity measurement: methods, materials and technologies, vol. 1: Spectroscopic methods of humidity measurement. Boca Raton: CRC Press; 2018.

32. Korotcenkov G. Handbook of humidity measurement: methods, materials and technologies, vol. 2: Electronic and electrical humidity sensors. Boca Raton: CRC Press; 2019.

33. Korotcenkov G. Handbook of humidity measurement: methods, materials and technologies, vol. 3: Sensing materials and technologies. Boca Raton: CRC Press; 2020.

34. Korotcenkov G. Current trends in nanomaterials for metal oxide-based conductometric gas sensors: advantages and limitations. Part 1: 1D and 2D nanostructures. Nanomaterials. 2020;10:1392.

35. Kulwick BM. (1991) Humidity sensors. J Am Ceram Soc. 1991;74(4):697–708.

36. Leung YP, Choy WCH, Yuk TI. Linearly resistive humidity sensor based on quasi one-dimensional ZnSe nanostructures. Chem Phys Lett. 2008;457:198–201.

37. Liang Y-C, Liu S-L. Synthesis and enhanced humidity detection response of nanoscale Au-particle-decorated ZnS spheres. Nanoscale Res Lett. 2014;9:647.

38. Lim HJ, Saha T, Tey BT, Tan WS, Ooi CW. Quartz crystal microbalance-based biosensors as rapid diagnostic devices for infectious diseases. Biosens Bioelectron. 2020;168(15):112513.

39. Long X, Chen J, Chen Y. Adsorption of ethyl xanthate on ZnS(110) surface in the presence of water molecules: a DFT study. Appl Surf Sci. 2016;370:11–8.

40. Lu T, Zhang M, Guo S, Liu R. Humidity and salt sensor based on CdSSe nanowire chip. IOP Conf Series: Mater Sci Eng. 2019;569:022006.

41. Luo M, Shao K, Long Z, Wang L, Peng C, Ouyang J, Na N. A paper-based plasma-assisted cataluminescence sensor for ethylene detection. Sens Actuators B Chem. 2017;240:132–41.

42. McCafferty E, Zettlemoyer AC. Adsorption of water vapour on α-Fe_2O_3. Faraday Discuss. 1971;52:239–54.

43. Moromoto T, Nagao M, Tokuda F. Relation between the amounts of chemisorbed and physisorbed water on metal oxides. J Phys Chem. 1969;73:243–8.

44. Muhammad F, Tahir M, Zeb M, Wahab F, Kalasad MN, Khan DN, Karimov KS. Cadmium selenide quantum dots: synthesis, characterization and their humidity and temperature sensing properties with poly-(dioctylfluorene). Sens Actuators B Chem. 2019;285:504–12.

45. Niarchos G, Dubourg G, Afroudakis G, Georgopoulos M, Tsouti V, Makarona E, Crnojevic-Bengin V, Tsamis C. Humidity sensing properties of paper substrates and their passivation with ZnO nanoparticles for sensor applications. Sensors. 2017;17:516.

46. Nitta T. Ceramic humidity sensor. Ind Eng Chem Prod Res Dev. 1981;20:669–74.

47. Okur S, Uzar N, Tekguzel N, Erol A, Arıkan MC. Synthesis and humidity sensing analysis of ZnS nanowires. Phys E. 2012;44:1103–7.

48. Parangusan H, Bhadra J, Ahmad Z, Mallick S, Touati F, Al-Than N. Capacitive type humidity sensor based on PANI decorated Cu-ZnS porous microspheres. Talanta. 2020;219:121361.

49. Ponec V, Knor Z, Cerný S. Adsorption on solids. London: Butterworth; 1974. p. 405.

50. Rittersma ZM. Recent achievements in miniaturised humidity sensors–a review of transduction techniques. Sens Actuators A Phys. 2002;96:196–210.

51. Sager K, Schroth A, Nakladal A, Gerlach G. Humidity-dependent mechanical properties of polyimide films and their use for IC-compatible humidity sensors. Sensors Actuators A Phys. 1996;53:330–4.

52. Sauerbrey G. The use of quartz oscillators for weighing thin layers and for microweighing. Z Phys. 1959;155:206–22.

53. Spomer LA, Tibbitts TW. Humidity. In: Langhans RW, Tibbitts TW, editors. Plant growth chamber handbook. Ames: Iowa State University; 1997. p. 43–64.

54. Srivastava R. Humidity sensor: an overview. Int J Green Nanotechnol. 2012;4:302–9.

55. Turkdogan S. Bandgap engineered II–VI quaternary alloys and their humidity sensing performance analyzed by QCM. J Mater Sci Mater Electron. 2019;30:10427–34.

56. Üzar N, Okur S, Arikana MC. Investigation of humidity sensing properties of ZnS nanowires synthesized by vapor liquid solid (VLS) technique. Sens. Actuators A. 2011;167:188–93.

57. Vashist SK, Vashist P. Recent advances in quartz crystal microbalance-based sensors. J Sensors. 2011;2011:571405.

58. Visscher GJW. Chapter 72: Humidity and moisture measurement. In: Webster JG, editor. The measurement, instrumentation, and sensors: handbook. Boca Raton: CRC; 1999.

59. Wiederhold PR. Water vapor measurement: methods and instrumentation. New York: CRC Press; 1997.
60. Wang M, Zhang Q, Hao W, Sun Z-X. Surface stoichiometry of zinc sulfide and its effect on the adsorption behaviors of xanthate. Chem Cent J. 2011;5:73.
61. Yan W, Hu C, Xi Y, Wan B, He X, Zhang M, Zhang Y. ZnSe nanorods prepared in hydroxide-melts and their application as a humidity sensor. Mater Res Bull. 2009;44:1205–8.
62. Zhang H, Gilbert B, Huang F, Banfield JF. Water-driven structure transformation in nanoparticles at room temperature. Nature. 2003;424:1025–9.
63. Zhang H, Rustad JR, Banfield JF. Interaction between water molecules and zinc sulfide nanoparticles studied by temperature-programmed desorption and molecular dynamics simulations. J Phys Chem A. 2007;111:5008–14.
64. Zhang M, Guo S, Weller D, Hao Y, Wang X, Ding C, et al. CdSSe nanowire-chip based wearable sweat sensor. J Nanobiotechnology. 2019;17:42.